

# Manganese Oxydiacetate Complexes: Synthesis, Structure and Magnetic Properties

Abdessamad Grirrane,<sup>[a]</sup> Antonio Pastor,<sup>[a]</sup> Eleuterio Álvarez,<sup>[b]</sup> Carlo Mealli,<sup>[c]</sup> Andrea Ienco,<sup>[c]</sup> Patrick Rosa,<sup>[d]</sup> Francisco Montilla,<sup>[a]</sup> and Agustín Galindo\*<sup>[a]</sup>

**Keywords:** Manganese / Tridentate ligands / Coordination modes / Magnetic properties

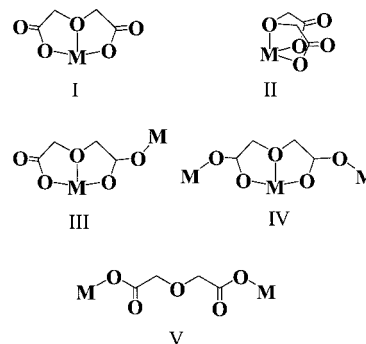
The aerobic aqueous solution syntheses and structures of monomeric and polymeric Mn<sup>II</sup> complexes containing the oxydiacetate ligand [O(CH<sub>2</sub>COO)<sub>2</sub><sup>2-</sup> = oda] are reported. The magnetic properties of the polymeric products have also been investigated. The initially obtained species [[Mn(oda)(H<sub>2</sub>O)]·H<sub>2</sub>O]<sub>n</sub> (**1**) has been reacted with bidentate or tridentate N-donor ligands such as *o*-phenanthroline (phen), 2,2'-bipyridine (bipy) and 2,2':6,2''-terpyridine (terpy) to give the complexes [[Mn(oda)(phen)]·4H<sub>2</sub>O]<sub>n</sub> (**2**), [Mn(oda)(bipy)(H<sub>2</sub>O)]·2H<sub>2</sub>O (**3**) and [Mn(oda)(terpy)]·2H<sub>2</sub>O (**4**), respectively. Species **1**–**4** are the first Mn-oda structures determined by X-ray methods. In all cases, the oda acts as a tridentate ligand toward one metal and adopts the typical planar arrangement. However, while the **3** and **4** are monomers, **2** and **1** are polymers as oda exploits both atoms of its carboxylate groups to coordinate other metals; **1** consists of

a three-dimensional diamond-type network, while **2** is one-dimensional, consisting of an extended chain of {Mn(oda)(phen)} subunits. For both compounds, magnetic susceptibility measurements down to 2 K showed only weak antiferromagnetic interactions between high-spin Mn<sup>II</sup> ions. Despite the expected similar coordinating capabilities of N-donor ligands, the bipy complex **3** is a monomer with the six-coordination completed by one water ligand. The tridentate nature of simultaneously present oda and terpy ligands excludes the coordination of water in complex **4**, the geometry of which is distorted from the octahedron, most likely due to a peculiar packing effect. Finally, the known five-coordinate complex [MnCl<sub>2</sub>(terpy)] (**5**), a side product of our synthetic experiments, has also been structurally characterized. (© Wiley-VCH Verlag GmbH & Co. KGaA, 69451 Weinheim, Germany, 2004)

## Introduction

As the active sites of several mononuclear enzymes are five- or six-coordinate manganese species containing coordinated carboxylate groups, water and nitrogen-donor molecules (for instance, imidazole groups),<sup>[1–5]</sup> research on the coordination compounds of manganese with such co-ligands has grown. In particular, model compounds may provide better insight into the manganese-based biological systems and, thus, most of this chemistry has been attempted in aqueous solution.

The oxydiacetate anion [oda = O(CH<sub>2</sub>COO)<sub>2</sub><sup>2-</sup>] features two carboxylate functions joined by a three-membered chain that is centred on an ethereal oxygen atom. The bonding capabilities of the ligand have been tested with



Scheme 1

most first-row transition metals, and mono-, bi- and poly-nucleating behaviours have been ascertained through several X ray structure determinations. Scheme 1 shows these coordination modes, without considering *syn* and *anti* isomers for the carboxylate bridge.

The ligand usually behaves as tridentate monometallic. Two possible isomers, I or II, are known, for which the ligand oda is overall planar<sup>[6–12]</sup> or puckered, respectively.<sup>[10,13,14]</sup> In six-coordinate complexes, these isomers are referred to as *mer* or *fac*, respectively. Our previous DFT

<sup>[a]</sup> Departamento de Química Inorgánica, Universidad de Sevilla, Aptdo. 553, 41071 Sevilla, Spain  
Fax: (internat.) + 34-95-4557153  
E-mail: galindo@us.es

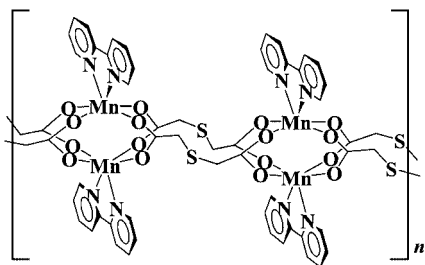
<sup>[b]</sup> Instituto de Investigaciones Químicas, CSIC, Avda. Américo Vespucio s/n, 41092 Sevilla, Spain

<sup>[c]</sup> ICCOM, CNR, Via Nardi 39, 50132 Firenze, Italy

<sup>[d]</sup> LAMM, Università degli Studi di Firenze, Via della Lastruccia 3, 50019 Sesto Fiorentino (FI), Italy

calculations for some nickel<sup>[12]</sup> and vanadium complexes,<sup>[15]</sup> as well as for the free oxydiacetic acid and the oxydiacetate anion,<sup>[12]</sup> all showed an energy difference between these isomers of a few kcal mol<sup>-1</sup>. The highest  $\Delta E$  of 8.5 kcal mol<sup>-1</sup> was found for the complex  $[\text{VO}(\text{oda})(\text{H}_2\text{O})_2]$ .<sup>[15]</sup> Our search in the Cambridge Database<sup>[16]</sup> on first row transition metals indicates that the most common binding mode for oda is planar (I in Scheme 1), with the external carboxylate oxygen atoms not involved in metal coordination. The residual nucleophilicity of the latter atoms is exerted usually through hydrogen bonding with crystallization water molecules.<sup>[6–12]</sup> There are other cases where the ligand oda still acts as tridentate toward one metal (in the overall planar arrangement), while the remaining carboxylate donors are also bound to one or two different metals (coordination modes III and IV, respectively, in Scheme 1). Two examples of these coordination modes are the complexes  $[\{\text{Co}(\text{oda})(\text{H}_2\text{O})_2\} \cdot \text{H}_2\text{O}]_n$ <sup>[17]</sup> and  $[\{\text{Zn}(\text{oda})\} \cdot 0.3\text{H}_2\text{O}]_n$ ,<sup>[9]</sup> respectively. Finally, in some cases the ethereal oxygen atom of oda is uncoordinated and the whole ligand acts a  $\mu$ -bridge between two equal metal centres, such as  $\text{Ti}^{\text{IV}}$ <sup>[7]</sup> and  $\text{Zn}^{\text{II}}$ ,<sup>[18]</sup> (structure V, Scheme 1). Despite the widespread use of oda as a ligand with first row transition metals, there is still a paucity of data relative to chromium and manganese metals and, in particular, neither structural nor conformational data are available. For instance, only a potentiometric study of a  $\text{Mn}^{\text{II}}$ -oda system has been reported, without any stereochemical implication for the nature of the adduct investigated.<sup>[19]</sup>

We have recently found an interesting behaviour of the thio- analogue of oda  $[\text{tda} = \text{S}(\text{CH}_2\text{COO})_2^{2-}]$  toward the  $\text{Mn}^{\text{II}}$  ion, with 2,2'-bipyridine as co-ligand. We have synthesized and documented the first example of a  $\text{Mn}^{\text{II}}$  dimer with the copper-acetate structure (sketch in Scheme 2).<sup>[20]</sup>  $[\text{Mn}(\text{tda})(\text{bipy})]_n$ , where the central sulfur atom of tda is not involved in coordination, is remarkable for at least three reasons: (i) the almost unobserved assembly of two local trigonal prisms through rectangular faces, (ii) the ascertained antiferromagnetism within the dimeric unit, (iii) the extended supramolecular arrangement formed in the solid state due to the interpenetration of the parallel bipyridine ligands in a gear-like arrangement. Encouraged by the above results, we have tested whether an aqueous solution of the ligand oda has an analogous reactivity pattern toward the  $\text{Mn}^{\text{II}}$  ion when associated with co-ligands such as 2,2'-bipyridine or other polydentate nitrogen bases. This



Scheme 2

chemistry is essentially unexplored and this paper presents the spectroscopic, magnetic and structural characterization of the synthesized products. The results are particularly interesting from the structural point of view as different stereochemical arrangements are observed for systems with components of similar nature.

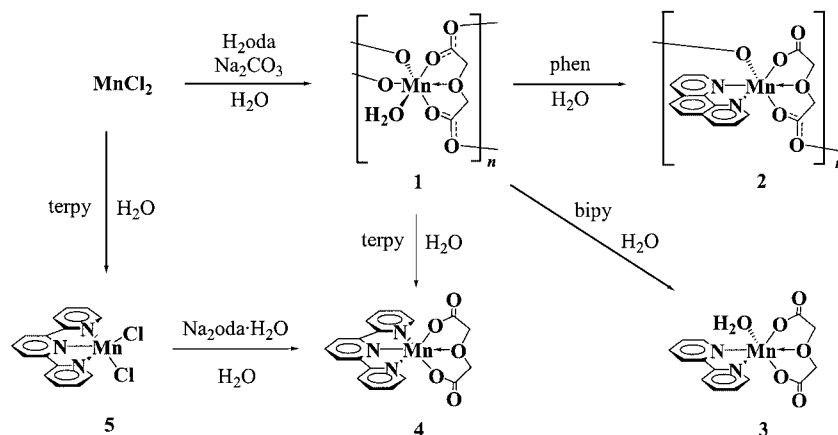
## Results and Discussion

A summary is given in Scheme 3 of the reactions and products studied. Beside routine spectroscopic analyses, the structures of compounds **1–5** have been determined by X-ray diffraction analysis. While species **1–4** represent the first examples of structurally characterized manganese oxydiacetate complexes, the oda-free compound **5** has been previously obtained,<sup>[21–23]</sup> and characterized by powder X-ray techniques<sup>[24]</sup> but its precise molecular structure was still unknown. All of the current work is illustrated in detail below.

### Synthesis and Characterization

Treatment of aerobic aqueous solutions of manganese dichloride with a 1:1 mixture of  $\text{Na}_2\text{CO}_3$  and oxydiacetic acid,  $\text{O}(\text{CH}_2\text{COOH})_2$ , affords, after work up, colourless crystals of complex  $[\text{Mn}(\text{oda})(\text{H}_2\text{O})_2]$  (**1**), in good yields. Related oxydiacetate complexes of nickel and cobalt were prepared by a similar procedure.<sup>[12]</sup> Only X-ray analysis (see below) could clearly show that **1** is a polymeric solid and that only one of the two water molecules is coordinated to the metal centre, so that the correct formulation is  $[\{\text{Mn}(\text{oda})(\text{H}_2\text{O})\} \cdot \text{H}_2\text{O}]_n$ . Subsequently, complex **1** was found react readily with each of three different N-donor ligands, *o*-phenanthroline (phen), 2,2'-bipyridine (bipy) and 2,2':6,2''-terpyridine (terpy) (Scheme 3), to give, almost invariably, good yields of yellow crystalline solids. Elemental analyses and the IR spectra indicated that additional water molecules were present in the so-obtained compounds but it was not possible to assess any difference between their coordination or simple crystallization roles. Again, only the subsequent X-ray determinations allowed us to assign formulae to the various products:  $[\{\text{Mn}(\text{oda})(\text{phen})\} \cdot 4\text{H}_2\text{O}]_n$  (**2**),  $[\text{Mn}(\text{oda})(\text{bipy})(\text{H}_2\text{O})] \cdot 2\text{H}_2\text{O}$  (**3**), and  $[\text{Mn}(\text{oda})(\text{terpy})] \cdot 2\text{H}_2\text{O}$  (**4**), respectively. Accordingly, while **3** and **4** are monomers, **2** is polymeric.

An alternative attempt to prepare complex **4** in a single step (i.e. by mixing in one pot  $\text{MnCl}_2$  with a 1:1 mixture of  $\text{Na}_2\text{CO}_3$  and  $\text{O}(\text{CH}_2\text{COOH})_2$  and by adding subsequently terpy) provided, after some work up, **4** and small amounts of a new yellow crystalline material that was analytically and structurally characterized as  $[\text{MnCl}_2(\text{terpy})]$  (**5**). Most probably, the obtainment of **5** was due to a small stoichiometric defect of  $\text{O}(\text{CH}_2\text{COOH})_2$  in the experimental procedure. In fact, as reported, complex **5** is easily obtainable by direct reaction between the water solutions of manganese dichloride with terpy.<sup>[21–23]</sup> Complex **4** is also formed from the reaction of the isolated complex **5** with one equivalent of sodium oxydiacetate (see Exp. Sect.). Evidently,



Scheme 3

species **5** is a sufficiently stable intermediate, which may or may not be isolated, in the reaction leading to **4**.

All of the synthesised compounds are air stable, both in solution and in the solid state. They may be dissolved in water but are not soluble in solvents of low polarity. The effective magnetic moments for **3** and **4** (solid state, room temperature) are in the range 5.7–5.9  $\mu_{\text{B}}$ , which are invariably consistent with five unpaired electrons in the ground-state configuration, and typical of high-spin mononuclear manganese(II) units. Similar manganese complexes that contain closely related ligands exhibit comparable  $\mu_{\text{B}}$  values {e.g. 5.95  $\mu_{\text{B}}$  for  $[\text{Mn}(\text{dipic})(\text{bipy})] \cdot 2\text{H}_2\text{O}$ ,  $\text{dipic} = \text{pyridine-2,6-dicarboxylate}$ }.<sup>[25]</sup> The magnetic behaviour of **1** and **2** is discussed below. Compounds **1–4** display the characteristic IR absorptions of oxydiacetate ligand. In particular, they feature a very strong, broad band at ca. 1600  $\text{cm}^{-1}$ , which corresponds to the antisymmetric vibrations of the carboxylate groups, and a strong band at ca. 1430  $\text{cm}^{-1}$ , which is assigned to the symmetric vibrations of the same groups. In many complexes of the first- and second-row<sup>[26,27]</sup> transition metals, and in all lanthanide and actinide complexes,<sup>[16]</sup> the ligand oda adopts a tridentate planar coordination mode. The non-planar arrangement of the ligand (**II** in Scheme 1) is uniquely found in some six-coordinate oxydiacetate compounds of nickel(II) and copper(II).<sup>[10,13,14]</sup> We have previously suggested and theoretically supported<sup>[12,15]</sup> the idea that the precise position of the C–O–C antisymmetric stretching band is diagnostic of the oda disposition in the various complexes. Thus, a planar oxydiacetate ligand is characterized by a sharp, strong band in the region 1150–1120  $\text{cm}^{-1}$ , while the active IR band falls in the region around 1100  $\text{cm}^{-1}$  when the arrangement is *fac*. Complexes **1–4** all display an absorption at ca. 1135  $\text{cm}^{-1}$  that is attributable to C–O–C antisymmetric stretching; hence the planar disposition of oda is invariably assumed, and, indeed, is confirmed by the X-ray structural determinations.

### Structural and Magnetic Studies

Compounds **1–5** have been structurally characterized by single-crystal X-ray diffraction analysis. In all cases, the

$\text{Mn}^{\text{II}}$  ion is high spin and, for **1–4**, the local coordination is pseudo-octahedral. Under these circumstances, the distribution of the five unpaired electrons in the 3d orbital shell is isotropic. Thus, the coordination bonds should be mainly due to the interaction of the ligands with the metal s and p orbitals, with a minor role for the d levels, as for  $d^0$  (main group metals) and  $d^{10}$  configurations, i.e. the crystal field stabilization energy has little influence in these complexes, which have a good degree of hypervalency. This view is supported by the easy deformation of complex **4** from the octahedron (vide infra), and the stabilization of the five-coordinate compound **5** further confirms the minor role of the d orbitals in fixing the coordination sphere.

As discussed in textbooks,<sup>[28]</sup> the ease of substitution of one water ligand in  $\text{Mn}^{\text{II}}$  and  $\text{Zn}^{\text{II}}$  octahedral complexes, with respect to the  $\text{Fe}^{\text{II}}$ ,  $\text{Co}^{\text{II}}$ ,  $\text{Ni}^{\text{II}}$  and  $\text{Cu}^{\text{II}}$  analogues (Irving–Williams series), can be related to the ratio between the charge and the effective ionic radius (Shannon type<sup>[29]</sup>). In particular, the high-spin  $\text{Mn}^{\text{II}}$  ion has the largest radius in the series. Direct comparison between some of the present manganese structures and their equivalents with other metals allows a further check of the trends indicated. For instance, the complex  $[\text{Mn}(\text{oda})(\text{bipy}) \cdot (\text{H}_2\text{O})] \cdot 2\text{H}_2\text{O}$  (**3**) has  $\text{Co}^{\text{II}}$ ,  $\text{Ni}^{\text{II}}$  and  $\text{Zn}^{\text{II}}$  analogues. Similarly,  $[\text{Mn}(\text{oda})(\text{terpy})] \cdot 2\text{H}_2\text{O}$  (**4**) can be usefully compared with the  $\text{Ni}^{\text{II}}$  and  $\text{Cu}^{\text{II}}$  species. Detailed information is provided below when discussing the single structures.

None of the  $\text{Mn}^{\text{II}}$  complexes with the ligand oda and other N-donor chelates exhibit the unique features of the thiodiacetate complex  $[\text{Mn}(\text{tda})(\text{bipy})]_n$  (Scheme 2), i.e. the two carboxylate functions of oda cannot be exploited to form a copper-acetate structural motif. This is probably because the affinity of the ethereal oxygen function for the manganese(II) ion is larger than with the thio-etheral counterpart. The apparently difficult formation of  $\text{Mn}^{\text{II}}-\text{S}_{\text{etheral}}$  bonds (there are only a few structurally documented examples<sup>[30–34]</sup>) favours the stretching of the tda chain and provides the best packing conditions to form the extended arrangement of the tetracarboxylate dimanganese units. Apparently, the  $\text{Mn}^{\text{II}}-\text{O}_{\text{etheral}}$  bond is readily

formed for  $\text{Mn}^{\text{II}}$ -oda, and the reactivity follows alternative routes.

### 3D-Polymeric Complex $\{[\text{Mn}(\text{oda})(\text{H}_2\text{O})]\cdot\text{H}_2\text{O}\}_n$ (**1**)

Each manganese(II) ion of the parent compound  $\{[\text{Mn}(\text{oda})(\text{H}_2\text{O})]\cdot\text{H}_2\text{O}\}_n$  (**1**) is six-coordinate by the tridentate oxydiacetate ligand in the *mer* configuration (planar arrangement), one coordinated water ligand and two additional oxygen atoms of carboxylic groups coming from symmetry repeated  $\{[\text{Mn}(\text{oda})(\text{H}_2\text{O})]\}$  units (Figure 1). In this manner all of the five oda oxygen atoms are engaged in donations to the metal (coordination mode IV in Scheme 1). The overall structure of **1** is evidently a polymer that extends in three dimensions due to the four connections (two incoming and two outgoing dative bonds) that each  $\{[\text{Mn}(\text{oda})(\text{H}_2\text{O})]\}$  fragment establishes with its neighbouring equivalents. Selected interatomic distances and angles for the local coordination of **1** are collected in Table 1. As usual, the Mn–O3 bond involving the ethereal oxygen atom [2.230(3) Å] is slightly longer than any other Mn–O(carboxylate) bond, either formed within one  $\{[\text{Mn}(\text{oda})(\text{H}_2\text{O})]\}$  unit [2.208(3) and 2.194(3) Å for Mn–O1 and Mn–O2, respectively] or in the combination of different units [2.114(3) and 2.182(3) Å, for Mn–O4' and Mn–O5'', respectively].

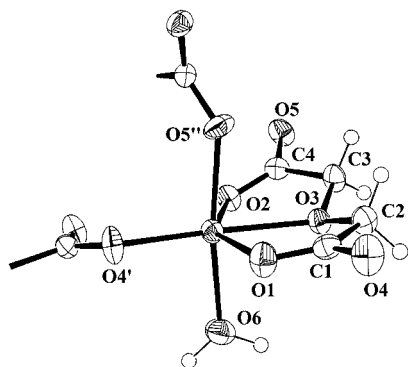


Figure 1. Local coordination environment about one  $\text{Mn}^{\text{II}}$  ion in  $\{[\text{Mn}(\text{oda})(\text{H}_2\text{O})]\cdot\text{H}_2\text{O}\}_n$  (**1**). The atoms labelled with ' and '' belong to two distinct  $\{[\text{Mn}(\text{oda})(\text{H}_2\text{O})]\}$  units repeated by the symmetry operations  $-x + 2, y - 1/2, -z + 3/2$  and  $x + 1/2, -y + 3/2, -z + 2$ , respectively.

The overall topology of the polymeric system is a diamond-like network that is not interpenetrated, according to the useful schemes of O'Keeffe and co-workers.<sup>[35]</sup> Figure 2 (a) shows a scheme of such an arrangement limited to the manganese atoms. The arbitrary connections between them show apparent cavities occupied by the oxygen atoms of the solvate water molecules. The hydrogen bonding network is a key feature for this and the other manganese oda complexes described here and deserves a detailed analysis. As stated by Perek and co-workers,<sup>[9]</sup> the hydrogen bonding network due to the coordinated and solvent water molecules fixes the crystal packing of most oxydiacetate metal complexes. Complex **1** has channels that are parallel to the *a* axis (Figure 2, b). Inside these channels, the solvent water molecules

Table 1. Selected bond lengths and angles for **1**

| Atoms <sup>[a]</sup> | Distance [Å] | Atoms       | Angle [°]  |
|----------------------|--------------|-------------|------------|
| Mn–O4'               | 2.114(3)     | O4'–Mn–O6   | 92.58(12)  |
| Mn–O6                | 2.173(3)     | O4'–Mn–O5'' | 94.88(12)  |
| Mn–O5''              | 2.182(3)     | O6–Mn–O5''  | 172.15(12) |
| Mn–O2                | 2.194(3)     | O4'–Mn–O2   | 120.39(10) |
| Mn–O1                | 2.208(3)     | O6–Mn–O2    | 91.61(11)  |
| Mn–O3                | 2.230(3)     | O5''–Mn–O2  | 86.74(10)  |
| O1–C1                | 1.235(4)     | O4'–Mn–O1   | 95.40(10)  |
| O2–C4                | 1.249(4)     | O6–Mn–O1    | 89.47(12)  |
| O3–C3                | 1.421(4)     | O5''–Mn–O1  | 87.38(11)  |
| O3–C2                | 1.423(4)     | O2–Mn–O1    | 144.09(9)  |
| O4–C1                | 1.266(4)     | O4'–Mn–O3   | 167.98(9)  |
| O5–C4                | 1.258(4)     | O6–Mn–O3    | 88.58(11)  |
| C1–C2                | 1.518(5)     | O5''–Mn–O3  | 83.62(10)  |
| C3–C4                | 1.511(5)     | O2–Mn–O3    | 71.51(9)   |
|                      |              | O1–Mn–O3    | 72.63(9)   |
|                      |              | C1–O1–Mn    | 118.7(2)   |
|                      |              | C4–O2–Mn    | 116.1(2)   |
|                      |              | C3–O3–C2    | 115.0(3)   |
|                      |              | C3–O3–Mn    | 115.4(2)   |
|                      |              | C2–O3–Mn    | 116.6(2)   |
|                      |              | C1–O4–Mn''' | 121.5(2)   |
|                      |              | C4–O5–Mn''' | 135.9(2)   |
|                      |              | O1–C1–O4    | 125.1(3)   |
|                      |              | O1–C1–C2    | 120.6(3)   |
|                      |              | O4–C1–C2    | 114.3(3)   |
|                      |              | O3–C2–C1    | 109.1(3)   |
|                      |              | O3–C3–C4    | 108.3(3)   |
|                      |              | O2–C4–O5    | 123.4(4)   |
|                      |              | O2–C4–C3    | 119.4(3)   |
|                      |              | O5–C4–C3    | 117.2(3)   |

<sup>[a]</sup> Symmetry transformations used to generate equivalent atoms: '  $-x + 2, y - 1/2, -z + 3/2$ ; ''  $x + 1/2, -y + 3/2, -z + 2$ ; '''  $-x + 2, y + 1/2, -z + 3/2$ ; ''''  $x - 1/2, -y + 3/2, -z + 2$ .

form a complicated structural pattern. For instance, the water molecule defined by O7 bridges two-coordinated water ligands (O6) of different  $\{[\text{Mn}(\text{oda})(\text{H}_2\text{O})]\}$  units. The O7...O6 separations are as long as 2.760(4) and 2.843(5) Å, respectively. Additionally, O7 is involved in hydrogen bonding with O2 and O4 of oda carboxylate groups [O7...O2 and O7...O4 of 2.896(4) and 2.853(4) Å, respectively].

The molar magnetic susceptibility of complex **1** was measured in the range 1.9–300 K. Both the susceptibility,  $\chi_{\text{mol}}$ , and its product with the temperature,  $\chi_{\text{mol}}T$ , (Figure 3) show typical paramagnetic behaviour. With 4.59 emu  $\text{K}\cdot\text{mol}^{-1}$  at 300 K,  $\chi_{\text{mol}}T$  is typical of uncorrelated high-spin  $\text{Mn}^{\text{II}}$  ions (theoretical value of 4.38  $\mu_{\text{B}}$  for five unpaired electrons and a Landé factor  $g = 2$ ). On lowering the temperature,  $\chi_{\text{mol}}T$  starts to decrease below 150 K, while  $\chi_{\text{mol}}$  rises monotonically to a maximum at 5 K, revealing weak antiferromagnetic interactions between the  $\text{Mn}^{\text{II}}$  centers. A plot of the inverse susceptibility  $1/\chi_{\text{mol}}$  versus temperature shows Curie–Weiss behaviour ( $1/\chi_{\text{mol}} = (T - \theta)/C$ ) with a Curie constant  $C = 4.705 \text{ emu K}\cdot\text{mol}^{-1}$  and  $\theta = -6.3 \text{ K}$ . The former magnitude corresponds to high-spin  $\text{Mn}^{\text{II}}$  with a  $g$ -factor of 2.074, which is far from the free-electron value expected for isotropic  $\text{Mn}^{\text{II}}$  and reflects experimental errors such as weighting. The  $\theta$  value can be accounted for by the mean-field model. As described by Kahn,<sup>[36]</sup>  $\theta = zJS(S + 1)/3k$ , where  $J$  is the interaction par-

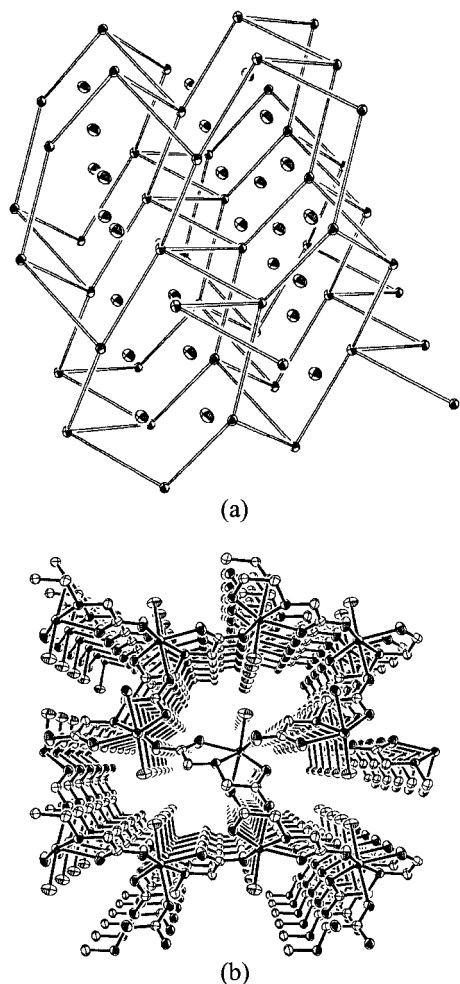


Figure 2. (a) Diamond-like three-dimensional pattern of  $[\{\text{Mn}(\text{oda})(\text{H}_2\text{O})\} \cdot \text{H}_2\text{O}]_n$  (**1**) as highlighted by the network of Mn atoms alone (the lines interconnecting these atoms are not bonds). Oxygen atoms of the crystallization water molecules are shown within the cavities. (b) Complete packing diagram down the *a* axis (crystallization water and hydrogen atoms excluded)

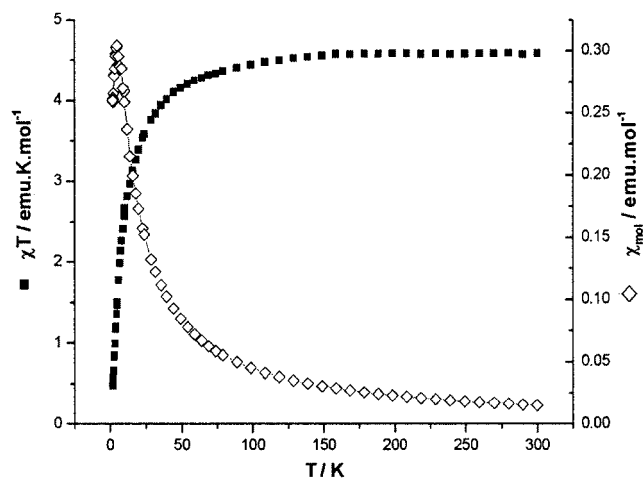


Figure 3. Molar magnetic susceptibility  $\chi_{\text{mol}}$  (◆, cgs units) and its product with the temperature,  $\chi_{\text{mol}}T$  (■, cgs units), of complex **1** between 1.9 and 300 K

ameter in the mean-field perturbation Hamiltonian  $\hat{H} = -zJ\langle\hat{S}_z\rangle\cdot\hat{S}_z$ , *S* is the spin of the interacting ion, and *z* is the number of nearest neighbours. For *z* = 4 (Figure 2, a) and *S* = 5/2, we find *J* = −0.19 cm<sup>−1</sup> for this polymeric system. This weak interaction is thus in the −0.193 to −0.30 cm<sup>−1</sup> range previously found for Mn<sup>II</sup> complexes that are similarly bridged by a unique carboxylate moiety.<sup>[37]</sup>

#### 1D-Polymeric Complex $[\{\text{Mn}(\text{oda})(\text{phen})\} \cdot 4\text{H}_2\text{O}]_n$ (**2**)

Compound **2** is also a polymer, in contrast with the related monomeric compounds  $[\text{M}(\text{oda})(\text{phen})(\text{H}_2\text{O})]$  (*M* = Ni,<sup>[10]</sup> Zn<sup>[9]</sup>). Each metal ion in **2** is six-coordinated by the three oxygen atoms of one oda ligand in the planar disposition, by the phen chelate and by an oxygen atom of a oda carboxylate group belonging to a symmetry repeated  $\{\text{Mn}(\text{oda})(\text{phen})\}$  unit (Figure 4, a). Here, the polymer extends as a one-dimensional chain (Figure 4, b) since each  $\{\text{Mn}(\text{oda})(\text{phen})\}$  unit acts both as an acceptor and as a donor with respect to its adjacent equivalents. The chains extend along the direction of the *a* axis. Selected bond lengths and angles for the local coordination of **2** are listed

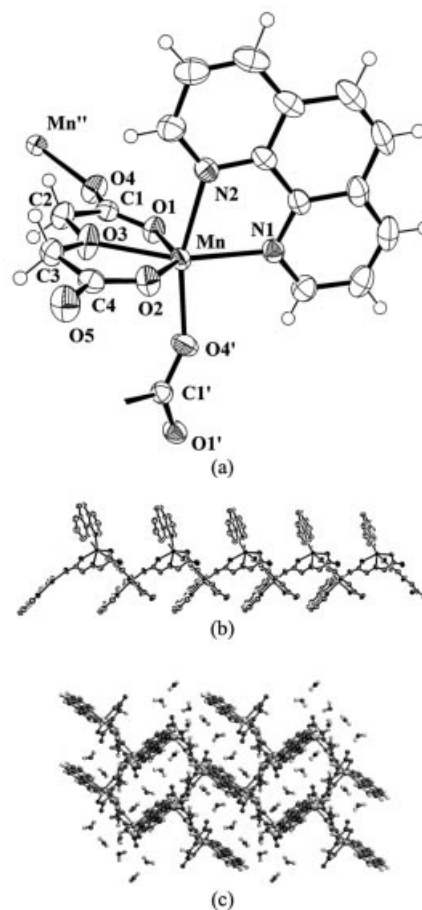


Figure 4. (a) Local coordination environment about Mn<sup>II</sup> ion in complex  $[\{\text{Mn}(\text{oda})(\text{phen})\} \cdot 4\text{H}_2\text{O}]_n$  (**2**). Primed and unprimed atoms are related by the symmetry operations *x*, *y*, *z* and *x*, 1/2 − *y*, *z*, respectively. (b) ORTEP drawing showing a portion of the extended chain of  $\{\text{Mn}(\text{oda})(\text{phen})\}$  units in **2**; interspersed H<sub>2</sub>O solvent molecules not shown. (c) View of the crystal packing of **2** that highlights the particular disposition of the solvent water molecules

Table 2. Selected bond lengths and angles for complexes 2–4

|                        | 2[a]       | 3          | 4          |
|------------------------|------------|------------|------------|
| Distances [Å]          |            |            |            |
| Mn–O1                  | 2.1798(17) | 2.156(2)   | 2.1149(14) |
| Mn–O2                  | 2.1680(17) | 2.185(2)   | 2.1501(13) |
| Mn–O3                  | 2.1876(17) | 2.195(2)   | 2.1727(15) |
| Mn–N1                  | 2.2184(19) | 2.245(3)   | 2.2611(16) |
| Mn–N2                  | 2.267(2)   | 2.242(3)   | 2.1950(15) |
| Mn–X <sup>[b]</sup>    | 2.1168(18) | 2.165(3)   | 2.2845(16) |
| O1–C1                  | 1.254(3)   | 1.253(3)   | 1.269(2)   |
| O2–C4                  | 1.262(3)   | 1.253(3)   | 1.259(2)   |
| O4–C1                  | 1.245(3)   | 1.249(3)   | 1.234(2)   |
| O5–C4                  | 1.241(3)   | 1.249(3)   | 1.237(2)   |
| O3–C2                  | 1.413(3)   | 1.416(3)   | 1.412(2)   |
| O3–C3                  | 1.417(3)   | 1.409(3)   | 1.404(2)   |
| C1–C2                  | 1.518(3)   | 1.515(4)   | 1.506(3)   |
| C3–C4                  | 1.513(3)   | 1.523(4)   | 1.513(3)   |
| Angles [°]             |            |            |            |
| O1–Mn–O2               | 142.73(6)  | 142.51(8)  | 142.87(5)  |
| O1–Mn–O3               | 71.03(6)   | 71.53(7)   | 72.18(5)   |
| O1–Mn–X <sup>[b]</sup> | 94.51(7)   | 99.29(10)  | 102.83(6)  |
| O2–Mn–O3               | 71.70(6)   | 70.99(8)   | 71.78(5)   |
| O2–Mn–X <sup>[b]</sup> | 93.25(7)   | 87.30(10)  | 91.30(6)   |
| O3–Mn–X <sup>[b]</sup> | 103.25(8)  | 98.87(9)   | 99.03(7)   |
| N1–Mn–N2               | 73.89(7)   | 72.35(9)   | 72.30(6)   |
| N1–Mn–O1               | 96.61(7)   | 96.01(8)   | 90.70(6)   |
| N1–Mn–O2               | 119.85(7)  | 121.17(8)  | 97.59(6)   |
| N1–Mn–O3               | 162.56(7)  | 166.36(8)  | 116.72(7)  |
| N1–Mn–X <sup>[b]</sup> | 89.66(7)   | 88.42(9)   | 144.19(6)  |
| N2–Mn–O1               | 95.68(7)   | 103.82(9)  | 120.34(5)  |
| N2–Mn–O2               | 87.93(7)   | 84.79(9)   | 96.59(6)   |
| N2–Mn–O3               | 94.64(8)   | 104.62(9)  | 165.64(6)  |
| N2–Mn–X <sup>[b]</sup> | 161.52(7)  | 151.17(10) | 72.25(6)   |

[a] Symmetry transformations used to generate equivalent atoms:  $x - 1/2, -y + 1/2, z$ . [b] The symbol "X" is atom O4', O6, and N3 for 2, 3, and 4, respectively.

in Table 2. Again, the coordination bond to the ethereal oxygen atom [Mn–O3 = 2.1876(17) Å] is slightly longer than any other Mn–O bond lengths. Amongst the latter, the distances within one {Mn(oda)(phen)} unit are longer than the corresponding inter-fragmental one [2.1680(17) and 2.1798(17) Å vs. 2.1168(18) Å, respectively]. There is no appreciable difference between the C–O bonds of the bidentate-dimetallic carboxylate group, but there is a minor asymmetry between the two C–O distances of the other carboxylate [compare the 1.241(3) and 1.262(3) Å for the C4–O5 and C4–O2 bonds, respectively]. At variance with 1, one carboxylate oxygen atom (O5) of oda remains unused for metal coordination (coordination mode III in Scheme 1).

As with complex 1, the hydrogen bonding network deserves a careful description. Solvent water molecules are interspersed between the parallel chains and participate to form a complicated hydrogen bonding network. In particular, the hydration molecules occupy the channels formed by the parallel disposition of the phenanthroline ligands (Figure 4, c). The carboxylate oxygen O5 forms two hydrogen bonds with two different water molecules centred at O7 and O9 [O5...O7 and O5...O9 are 2.812(3) and 2.851(3) Å, respectively]. A third water molecule (defined by O8)

bridges the two previous ones [O8...O7 and O8...O9 of 2.940(4) and 2.775(4) Å, respectively]. A fourth hydration molecule, centred at O6, makes a hydrogen bonding with that at O7 [H71...O6 and H61...O7 of 2.00(5) and 1.86(5) Å, respectively]. Finally, the network features two similarly weak interactions between one water molecule and one-coordinated oxygen atom of ligand oda. In fact, O6 is 2.920(3) Å from O1, and O9 is 2.952(3) Å from O2.

The temperature dependence of the molar magnetic susceptibility of complex 2 was also measured. Both the susceptibility,  $\chi_{\text{mol}}$ , and its product with the temperature,  $\chi_{\text{mol}}T$ , (Figure 5) again show typical paramagnetic behaviour. With 4.36 emu K·mol<sup>−1</sup> at 300 K, the  $\chi_{\text{mol}}T$  product corresponds to uncorrelated high-spin Mn<sup>II</sup> ions. On lowering the temperature,  $\chi_{\text{mol}}T$  starts to decrease below 50 K, while  $\chi_{\text{mol}}$  rises monotonically without reaching a maximum. Though there are clearly antiferromagnetic interactions between the Mn<sup>II</sup> centers, these are much weaker than those of complex 1. The plot of the inverse susceptibility  $1/\chi_{\text{mol}}$  versus temperature indicates Curie–Weiss behaviour with  $\theta = -1.9$  K, and the expected theoretical value  $C = 4.385$  emu K·mol<sup>−1</sup>. For  $z = 2$ , for this polymeric chained system (Figure 4, b), and  $S = 5/2$ , we obtain  $J = -0.11$  cm<sup>−1</sup> through the mean-field model. Although weaker, this value is still close to the range previously cited for similarly bonded complexes.

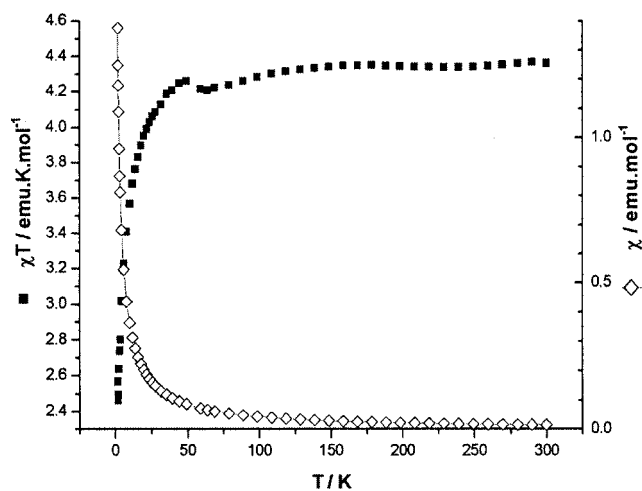


Figure 5. Molar magnetic susceptibility  $\chi_{\text{mol}}$  ( $\diamond$ , cgs units) and its product with the temperature,  $\chi_{\text{mol}}T$  ( $\blacksquare$ , cgs units), of complex 2 between 1.9 and 300 K

### Structure of [Mn(oda)(bipy)(H<sub>2</sub>O)]·2H<sub>2</sub>O (3)

Despite the expectedly similar coordinating capabilities of the phen and bipy ligands, the reaction of 1 with bipy affords the complex [Mn(oda)(bipy)(H<sub>2</sub>O)]·2H<sub>2</sub>O (3), which is monomer, in contrast to the polymeric character of 2. There are other examples of similar metal-carboxylate complexes whose different structural motifs are imposed by the nature of the N-donor co-ligand. For example, a manganese succinato derivative that is a dimer when coordinated with 1,10-phenanthroline<sup>[38,39]</sup> becomes polymeric (catena type) when 2,2'-bipyridine is used.<sup>[38–40]</sup> The manganese ion in 3

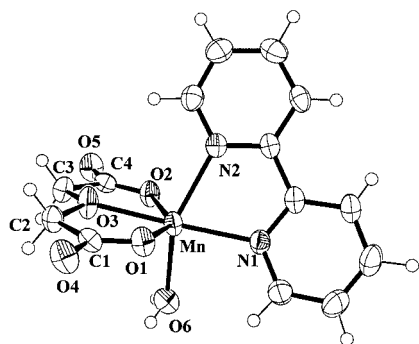


Figure 6. Molecular structure of the  $[\text{Mn}(\text{oda})(\text{bipy})(\text{H}_2\text{O})]\cdot 2\text{H}_2\text{O}$  complex (**3**); water molecules of crystallization not shown

is coordinated by the planar oxydiacetate anion, the bipy chelate and by one water molecule (Figure 6). The overall coordination mode is the most classic (I in Scheme 1) with only one oxygen atom per carboxylate group engaged as a donor towards the metal. Selected bond lengths and angles of complex **3** show no major differences in Mn-oda geometry compared with those of **2** (Table 2). However, even though only one oxygen atom per carboxylate is involved in metal coordination (O1 and O2), a delocalisation of the  $\pi$  bonding is observed, with all of the C–O distances being close to ca. 1.25 Å.

Although a monomer, compound **3** also has a peculiar hydrogen bonding network that certainly affects its crystal packing. The latter, described below, is certainly different from the one common to three isomorphous compounds that have the equivalent basic formula  $[\text{M}(\text{oda})(\text{bipy})(\text{H}_2\text{O})]$  ( $\text{M} = \text{Ni}^{[12]}$ ,  $\text{Co}^{[12]}$  and  $\text{Zn}^{[9]}$ ). In fact, they, with 2.5 crystallization water molecules, belong to the space group  $Fdd2$ , while **3**, with only two hydration molecules, crystallizes in  $P2_1/n$ . In **3**, the O7 of one solvent water molecule forms two hydrogen bonds with the uncoordinated O4 and O5 of two carboxylate groups [ $\text{O5}\cdots\text{O7}$  and  $\text{O4}\cdots\text{O7}$  contacts are 2.83(4) and 2.85(4) Å, respectively]. The second  $\text{H}_2\text{O}$  molecule, centred at O8, acts as an hydrogen bonding acceptor from the metal-coordinated  $\text{H}_2\text{O}$  molecule (O6), while it is a donor with respect to both the carboxylate O5 atom and the O7 water atom. The three contacts projecting from O8 are 2.68(4), 2.76(4) and 2.83(5) Å, respectively. The Mn–O and Mn–N distances in **3** are the longest in the  $[\text{M}(\text{oda})(\text{bipy})(\text{H}_2\text{O})]$  series, the order being  $\text{Mn}^{\text{II}} > \text{Zn}^{\text{II}} > \text{Co}^{\text{II}} > \text{Ni}^{\text{II}}$  (Table 3). As mentioned, the trend agrees with that of the Shannon radii and indirectly with the  $q/r$  ratios for these elements. The expanded coordination sphere of  $\text{Mn}^{\text{II}}$  also combines with larger distortions from the regular octa-

hedral geometry. In particular, the O6–Mn–N2 angle deviates from linearity [ $151.17(10)^\circ$ ], a feature that, for instance, is much less evident for the other derivatives [cf.  $170.4(1)^\circ$  for nickel,  $167.1(1)^\circ$  for cobalt and  $169.0(2)^\circ$  for zinc].

Finally, the overall geometry of **3** resembles that of the closely relatable mononuclear complex  $[\text{Mn}(\text{chedam})(\text{bipy})(\text{H}_2\text{O})]$  (chedam = 4-hydroxypyridine-2,6-dicarboxylate).<sup>[25]</sup> The greater *trans* influence of the nitrogen donor of chedam with respect to that of the ethereal O3 atom of oda is evident. In fact, the Mn–N1 of 2.245(3) Å in **3** is significantly shorter than the corresponding Mn–N of 2.278(1) Å in the complex with the ligand chedam.

#### Structure of $[\text{Mn}(\text{oda})(\text{terpy})]\cdot 2\text{H}_2\text{O}$ (**4**)

The crystal structure of six-coordinate complex **4** is composed of discrete  $[\text{Mn}(\text{oda})(\text{terpy})]$  units (Figure 7, a), plus two water molecules of crystallization. Selected bond lengths and angles are given in Table 2. The connectivity requirements of both the oda and terpy ligands, both tridentate and planar arranged, prevents bite angles of  $90^\circ$  for any of the adjacent N–Mn–N or O–Mn–O. Accordingly, the geometry of the compounds is far from a regular octahedron. Moreover, the structure is distorted also from its highest possible symmetrical arrangement where the two oda and terpy planes could act as reciprocal mirror planes. These planes are still roughly almost perpendicular [the angle between the mean square planes is ca.  $84.21(4)^\circ$ ] but the terpy molecule is significantly bent toward one of the lateral oxygen donors of oda (O2). Consider, for instance, the large difference between O2–Mn–N2 [ $96.59(6)^\circ$ ] and O1–Mn–N2 [ $120.34(5)^\circ$ ] (where N2 is the central donor of terpy). Interestingly, such a distortion does not seem to have an electronic origin but it is more likely due to the particular packing of  $[\text{Mn}(\text{oda})(\text{terpy})]$  molecules in the crystal. Figure 7 (b) shows that two terpy ligands of different molecules are clearly parallel (the planes are ca. 3.7 Å apart), but their  $\pi$  stacking involves only two of the three six-membered rings. Namely, only one central and one lateral ring of one terpy ligand eclipse precisely the equivalent rings of the other complex molecule. Furthermore, intermolecular hydrogen bonding also occurs (Figure 7, b). Generally, C–H groups of aromatic rings are not excellent hydrogen-bonding donors, but here one metal-coordinated carboxylate oxygen atom seems to be able to form such a bond [ $\text{O2}\cdots\text{H13}'' = 2.46(1)$  Å], and so causes the asymmetric orientation of oda, which should have a low energetic cost. This distortion is not so evident in the similar Ni and Cu complexes  $[\text{M}(\text{oda})(\text{terpy})]$ . In addition, these structures crystallize in different space groups ( $P2_1/n$  and  $P2_1/c$ , respectively) and, as pointed out for **3**, the crystal packing and hydrogen bonding networks are, consequently, different. In particular, in **4** one lattice water molecule (O7) forms hydrogen bonds with the uncoordinated carboxylate oxygens O4 and O5 of two symmetry related  $[\text{Mn}(\text{oda})(\text{terpy})]$  molecules [ $\text{O7}\cdots\text{O4}$  and  $\text{O7}\cdots\text{O5}$  of 2.76(3) and 2.84(3) Å, respectively]. The second water molecule defined by O6 bridges, through two hydrogen bonds, the carboxylate oxy-

Table 3. Comparison of selected bond lengths (Å) around the metal centre in  $[\text{M}(\text{oda})(\text{bipy})(\text{H}_2\text{O})]$  complexes

| M    | Mn       | Ni <sup>[12]</sup> | Co <sup>[12]</sup> | Zn <sup>[9]</sup> |
|------|----------|--------------------|--------------------|-------------------|
| M–O1 | 2.156(2) | 2.055(3)           | 2.050(3)           | 2.054(6)          |
| M–O2 | 2.185(2) | 2.054(3)           | 2.096(3)           | 2.084(5)          |
| M–O3 | 2.195(2) | 2.042(2)           | 2.115(3)           | 2.160(5)          |
| M–N1 | 2.245(3) | 2.046(3)           | 2.096(3)           | 2.102(5)          |
| M–N2 | 2.242(3) | 2.067(3)           | 2.115(3)           | 2.145(6)          |

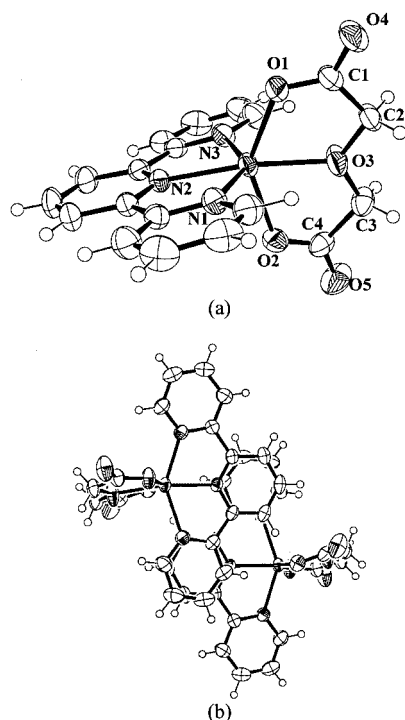


Figure 7. (a) Complex  $[\text{Mn}(\text{oda})(\text{terpy})]\cdot 2\text{H}_2\text{O}$  (**4**) (water molecules of hydration not shown). (b) Packing diagram of two symmetry related  $[\text{Mn}(\text{oda})(\text{terpy})]$  molecules, highlighting the hydrogen interaction

gens O1 and O5 of two  $[\text{Mn}(\text{oda})(\text{terpy})]$  units  $[\text{O6}\cdots\text{O1}$  and  $\text{O6}\cdots\text{O5}$  of 2.86(3) and 2.88(2) Å, respectively].

The bond to the ethereal oxygen atom  $[\text{Mn}-\text{O3}$ , 2.1727(15) Å] is again longer than the other two  $\text{Mn}-\text{O1}$  and  $\text{Mn}-\text{O2}$  lengths [2.1149(14) and 2.1501(14) Å, respectively]. This fact, although general for the manganese complexes discussed here, is in contrast with the equivalent structures of  $\text{Ni}^{\text{II}}$  [10] and  $\text{Cu}^{\text{II}}$  [6] ions (Table 4). In fact, the latter exhibit shorter  $\text{M}-\text{O}_{\text{ether}}$  bonds than the other two  $\text{M}-\text{O}$  distances. Also, the  $\text{Mn}-\text{N}$  lengths in **4** are longer than the similar  $\text{M}-\text{N}$  in the Ni and Cu complexes, in agreement with the larger effective ionic radii,<sup>[29]</sup> as previously discussed.

Table 4. Comparison of selected bond lengths (Å) around the metal centre in  $[\text{M}(\text{oda})(\text{terpy})]$  complexes

| M    | Mn         | Ni <sup>[10]</sup> | Cu <sup>[6]</sup> |
|------|------------|--------------------|-------------------|
| M–O1 | 2.1149(14) | 2.067(2)           | 2.202(5)          |
| M–O2 | 2.1501(13) | 2.074(2)           | 2.312(5)          |
| M–O3 | 2.1727(15) | 2.014(2)           | 2.070(5)          |
| M–N1 | 2.2611(16) | 1.985(3)           | 1.942(3)          |
| M–N2 | 2.1950(15) | 2.097(3)           | 2.031(4)          |
| M–N3 | 2.2845(16) | 2.105(3)           | 2.039(3)          |

### Structure of $[\text{MnCl}_2(\text{terpy})]$ (**5**)

As mentioned, the complex  $[\text{MnCl}_2(\text{terpy})]$  (**5**) has been previously reported,<sup>[21–23]</sup> and characterized by powder X-ray techniques,<sup>[24]</sup> but its molecular structure was unknown. Here, we observed that the manganese atom is five-coordi-

nate and that the overall geometry is a distorted square pyramid (Figure 8). The only other example of a pentacoordinate manganese complex containing the terpy ligand is the compound  $[\text{Mn}(2,6\text{-dimethoxybenzoato-}O)_2(\text{terpy})]$ .<sup>[41]</sup>

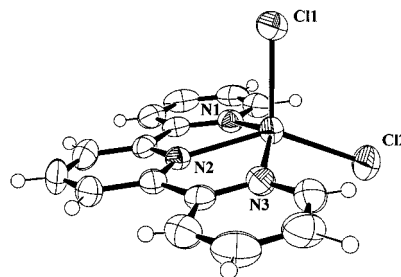


Figure 8. Molecular structure of  $[\text{MnCl}_2(\text{terpy})]$  (**5**)

Selected bond lengths and angles of **5** are collected in Table 5. The  $\text{Mn}-\text{Cl}$  are similar [2.3611(15) and 2.3452(14) Å], whereas the three  $\text{Mn}-\text{N}$  compares well with those in complex **4**. The other structural parameters do not require further comments because they are unexceptional.

Table 5. Selected bond lengths and angles for **5**

| Atoms   | Distance [Å] | Atoms       | Angle [°]  |
|---------|--------------|-------------|------------|
| Mn1–Cl1 | 2.3611(15)   | N2–Mn1–N1   | 72.07(12)  |
| Mn1–Cl2 | 2.3452(14)   | N2–Mn1–N3   | 71.90(13)  |
| Mn1–N1  | 2.256(4)     | N1–Mn1–N3   | 141.93(13) |
| Mn1–N2  | 2.203(3)     | N2–Mn1–Cl2  | 144.16(10) |
| Mn1–N3  | 2.268(4)     | N1–Mn1–Cl2  | 104.34(10) |
|         |              | N3–Mn1–Cl2  | 97.66(10)  |
|         |              | N2–Mn1–Cl1  | 104.71(9)  |
|         |              | N1–Mn1–Cl1  | 97.79(10)  |
|         |              | N3–Mn1–Cl1  | 102.79(10) |
|         |              | Cl2–Mn1–Cl1 | 111.07(5)  |

### Conclusion

We have reported  $\text{Mn}^{\text{II}}$ -oda chemistry not previously explored. Four different types of compounds have been obtained and characterized that indicate the great propensity of this ligand to stabilize both monomeric and polymeric solid state compounds. Obviously, their characterization has required systematic X-ray diffraction studies that have allowed us to confirm the precise structural arrangements and also the easily deformable coordination sphere about the high-spin manganese(II) ion. The structural studies have highlighted the hydrogen bonding interactions in all the oda complexes studied, involving both the coordinated and the lattice water molecules and carboxylate oxygen atoms of oxydiacetate. These interactions may be fundamental in determining the crystal packing of various oda compounds. In particular, some of the manganese complexes have the same coordination sphere as other previously reported first-row transition metal compounds, but the overall crystal properties are different. Finally, the determined antiferromagnetic coupling constants for the present  $\text{Mn}^{\text{II}}$ -oda poly-

meric systems are very small and fall in the lowest range reported for related carboxylate-bridged Mn<sup>II</sup> complexes.<sup>[37]</sup>

## Experimental Section

**General Remarks:** All preparations and other operations were carried out under aerobic conditions. Microanalyses (C, H, N) were carried out by the Microanalytical Service of the Instituto de Investigaciones Químicas (CSIC). Infrared spectra were recorded with a Perkin-Elmer Model 883 spectrophotometer (Nujol emulsion in NaCl plates). Magnetic moments were measured in the solid state, at room temperature, with a Sherwood Scientific (Cambridge Research Laboratory) magnetic balance, and between 1.9 and 300 K with a Cryogenic S600 SQUID magnetometer. Molar susceptibilities were then corrected using Pascal's constants.<sup>[42]</sup> Oxydiacetic acid and other chemicals were obtained from commercial sources and were used without further purification. The experimental procedure for the synthesis of **5** has also been included, although its preparation has been reported previously.<sup>[21–23]</sup>

**[{Mn(oda)(H<sub>2</sub>O)}·H<sub>2</sub>O]<sub>n</sub> (1):** Na<sub>2</sub>CO<sub>3</sub> (1.28 g, 12 mmol) was added to a solution of O(CH<sub>2</sub>COOH)<sub>2</sub> (1.61 g, 12 mmol) in water (20 mL). The mixture was then stirred until the evolution of CO<sub>2</sub> ceased and then added to a solution of MnCl<sub>2</sub>·4H<sub>2</sub>O (2.37 g, 12 mmol) in water (25 mL). The resulting solution was stirred for 15 minutes and then concentrated. Acetone was added and the solution was then kept at room temperature overnight. Colourless crystals of complex **1** were formed, filtered off, washed with acetone and Et<sub>2</sub>O and air dried (1.80 g, 65 %). IR (cm<sup>-1</sup>):  $\tilde{\nu}$  = 3350 br.  $\nu$ (OH), 1587 s br.  $\nu$ (COO<sub>asym.</sub>), 1431 s  $\nu$ (COO<sub>sym.</sub>), 1137 s  $\nu$ (CO-C<sub>asym.</sub>).  $\mu$  = 5.8  $\mu_B$  at 24 °C. C<sub>4</sub>H<sub>8</sub>MnO<sub>7</sub> (223.04): calcd. C 21.52, H 3.59; found C 21.43, H 3.62.

**[{Mn(oda)(phen)}·4H<sub>2</sub>O]<sub>n</sub> (2):** A solution containing *o*-phenanthroline·H<sub>2</sub>O (0.10 g, 0.5 mmol) in hot water (20 mL) was added to a solution of **1** (0.12 g, 0.5 mmol) in water (15 mL). The resulting solution was then stirred for a few minutes. Subsequently, compound **2** crystallized upon evaporation of the solvent at room temperature after a few days; yellow crystals were filtered off, washed with water and acetone and dried in air (0.15 g, 70 %). IR (cm<sup>-1</sup>):  $\tilde{\nu}$  = 3478, 3368 br.  $\nu$ (OH), 1601 s br.  $\nu$ (COO<sub>asym.</sub>), 1431 s  $\nu$ (COO<sub>sym.</sub>), 1137 s  $\nu$ (COC<sub>asym.</sub>).  $\mu$  = 5.7  $\mu_B$  at 24 °C. C<sub>16</sub>H<sub>20</sub>MnN<sub>2</sub>O<sub>9</sub> (439.28): calcd. C 43.73, H 4.55, N 6.38; found C 43.81, H 4.60, N 6.74.

**[Mn(oda)(bipy)(H<sub>2</sub>O)]·2H<sub>2</sub>O (3):** Following a similar synthetic procedure as described for compound **2**, but using **1** (0.48 g, 2 mmol) and bipy (0.31 g, 2 mmol), **3** was obtained as yellow crystals in 70 % yield. IR (cm<sup>-1</sup>): 3359 br.  $\nu$ (OH), 1601 s br.  $\nu$ (COO<sub>asym.</sub>), 1449 s  $\nu$ (COO<sub>sym.</sub>), 1137 s  $\nu$ (COC<sub>asym.</sub>).  $\mu$  = 5.7  $\mu_B$  at 22 °C. C<sub>14</sub>H<sub>18</sub>MnN<sub>2</sub>O<sub>8</sub> (397.24): calcd. C 42.32, H 4.53, N 7.05; found C 41.87, H 4.61, N 7.17.

**[Mn(oda)(terpy)]·2H<sub>2</sub>O (4):** A solution of **1** (0.12 g, 0.5 mmol) in water (20 mL) was added to a suspension of terpy (0.12 g, 0.5 mmol) in water (30 mL). The mixture was then stirred until all the solid was dissolved and then it was concentrated. Slow evaporation of water afforded yellow crystals of **4**, which were collected by filtration, washed with water, acetone and diethyl ether and dried (0.18 g, 80 %). Re-crystallization of the product in water yielded yellow crystals suitable for an X-ray study. IR (cm<sup>-1</sup>):  $\tilde{\nu}$  = 3533, 3432, 3350 br.  $\nu$ (OH), 1614 s br.  $\nu$ (COO<sub>asym.</sub>), 1426 s  $\nu$ (CO-O<sub>sym.</sub>), 1133 s  $\nu$ (COC<sub>asym.</sub>).  $\mu$  = 5.9  $\mu_B$  at 24 °C. C<sub>19</sub>H<sub>19</sub>MnN<sub>3</sub>O<sub>7</sub> (456.31): calcd. C 49.97, H 4.16, N 9.2; found C 49.96, H 4.27, N

9.30. As an alternative route to this complex a solution of O(CH<sub>2</sub>COONa)<sub>2</sub>·H<sub>2</sub>O (0.03 g, 0.15 mmol) in water (5 mL) was added to a solution of [MnCl<sub>2</sub>(terpy)] (**5**) (0.05 g, 0.15 mmol) in water (10 mL). The resultant mixture was then stirred for 3 h. Slow evaporation of the solvent then gave yellow crystals of **4**, which were collected by filtration and air dried (0.03 g; 45 %).

**[MnCl<sub>2</sub>(terpy)] (5):** A suspension of terpy (0.24 g, 1 mmol) in water (10 mL) was added to a solution of MnCl<sub>2</sub>·4H<sub>2</sub>O (0.20 g, 1 mmol) in water (10 mL). The mixture was then stirred until a yellow solution formed, which was then concentrated. Yellow crystals of compound **5** were obtained after slow evaporation of the solvent (0.27 g, 75 %). C<sub>15</sub>H<sub>11</sub>Cl<sub>2</sub>MnN<sub>3</sub> (359.12): calcd. C 50.12, H 3.06, N 11.69; found C 48.35, H 3.03, N 11.38.

**X-ray Crystallographic Study:** The crystal data and structural refinement of compounds **1–5** are summarized in Table 6. While the X-ray data of compound **1** were collected on a Bruker SMART diffractometer equipped with a 6000 CCD detector, all other data sets were collected on an Enraf–Nonius CAD4 diffractometer. Therefore, two distinct descriptions of the technical details are given.

In addition to the 6000 CCD detector, the Bruker SMART apparatus is equipped with a rotating anode generator, Goebel optics monochromated Cu-K $\alpha$  radiation ( $\lambda$  = 1.54178 Å), and a Kryoflex low-temperature device.<sup>[43]</sup> Six sets of frames covering a hemisphere of the reciprocal space were recorded for a well-formed crystal of **1** (3 × 600 frames to  $\phi$  = 0°, 120° and 240° respectively with the CCD detector placed to  $2\theta$  = -40°, and others 3 × 600 frames to  $\phi$  = 60°, 180° and 300° respectively with the CCD detector placed to  $2\theta$  = -100°,  $\omega$ -scans,  $\Delta\omega$  = 0.3°, time per frame 5 s). Data reduction up to  $\theta$  = 81° was performed with the program SAINT+, and corrections for absorption with SADABS; of 4361 reflections measured 1417 were independent,  $R_{\text{int}}$  = 0.063.<sup>[43]</sup> The structure was solved by direct methods and refined by full-matrix least-squares on  $F^2$  using the program SHELXL-97.<sup>[44]</sup> All non-hydrogen atoms were refined with anisotropic displacement parameters. The hydrogen atoms were located on a difference Fourier map and refined with isotropic displacement parameters. The highest residual peaks (three) 0.70–0.69 e·Å<sup>-3</sup> were located close to the heavier atoms Mn and have no chemical sense.

Well-formed yellow crystals of the compounds **2–5** were mounted on a Enraf–Nonius CAD4 diffractometer equipped with a graphite monochromator and Mo-K $\alpha$  radiation ( $\lambda$  = 0.71073 Å). In all cases, the cell dimensions were refined by least-squares refinement of 25 reflections in the  $2\theta$  range 10–20°. The intensity data were corrected for Lorentz and polarization effects and semiempirical absorption corrections ( $\psi$  scan). Three standard reflections were monitored every two hours during data collection. Atomic scattering factors are those reported by Cromer and Waber.<sup>[45]</sup> The structures were solved by direct methods using the SIR97<sup>[46]</sup> package of programs. Refinements were made by full-matrix least-squares on all  $F^2$  data using SHELXL-97.<sup>[44]</sup> In general,  $\Delta F$  Fourier maps, calculated at a later stage of refinement, allowed the localization of the hydrogen atoms. These atoms were assigned isotropic temperature factors and were refined in the final least-squares cycles. Anisotropic thermal parameters were allotted to all of the non-hydrogen atoms. No unusual trend in  $\Delta F$  vs.  $F_o$  or  $(\sin\theta)/\lambda$  was observed. In no case was a significant electron density residue detected from the final  $\Delta F$  maps.

The molecular drawings were made using the program ORTEP-III for Windows<sup>[47,48]</sup> and SCHAKAL (Figure 3, c).<sup>[49]</sup> All crystallographic computational work was performed by using the user-friendly graphic interface of WINGX.<sup>[50]</sup>

Table 6. Crystallographic data for complexes 1–5

|   | 1   | 2   | 3   | 4   | 5  |
|---|---|---|---|---|--|
| Empirical formula   | C <sub>4</sub> H <sub>8</sub> MnO <sub>7</sub>            | C <sub>16</sub> H <sub>20</sub> MnN <sub>2</sub> O <sub>9</sub> | C <sub>14</sub> H <sub>18</sub> MnN <sub>2</sub> O <sub>8</sub> | C <sub>19</sub> H <sub>19</sub> MnN <sub>3</sub> O <sub>7</sub> | C <sub>15</sub> H <sub>11</sub> Cl <sub>2</sub> MnN <sub>3</sub> |
| Molecular mass  | 223.04  | 439.28  | 397.24  | 456.31  | 359.11   |
| Crystal system  | orthorhombic  | monoclinic  | monoclinic  | triclinic   | monoclinic   |
| Space group   | <i>P</i> 2 <sub>1</sub> 2 <sub>1</sub> 2 <sub>1</sub> [a] | <i>P</i> 2 <sub>1</sub> / <i>a</i>                              | <i>P</i> 2 <sub>1</sub> / <i>n</i>                              | <i>P</i> 1bar   | <i>P</i> 2 <sub>1</sub> / <i>c</i>                               |
| <i>a</i> [Å]  | 6.9643(2)   | 9.639(4)  | 6.895(5)  | 8.5860(10)  | 10.9596(19)  |
| <i>b</i> [Å]  | 9.9724(3)   | 18.144(2)   | 24.361(7)   | 10.5680(10)   | 8.232(4)   |
| <i>c</i> [Å]  | 11.1951(3)  | 10.7654(11)   | 10.1538(13)   | 11.405(3)   | 16.289(3)  |
| $\alpha$ [°]  | 90  | 90  | 90  | 79.38(2)  | 90   |
| $\beta$ [°]   | 90  | 95.633(19)  | 100.72(2)   | 82.360(10)  | 94.024(14)   |
| $\gamma$ [°]  | 90  | 90  | 90  | 75.040(10)  | 90   |
| Volume [Å <sup>3</sup> ]  | 777.51(4)   | 1873.6(8)   | 1675.8(15)  | 978.7(3)  | 1465.9(7)  |
| <i>Z</i>  | 4   | 4   | 4   | 2   | 4  |
| Calculated density [g cm <sup>-3</sup> ]                            | 1.905   | 1.557   | 1.575   | 1.548   | 1.627  |
| Absorption coefficient (Mo- <i>K</i> $\alpha$ ) [mm <sup>-1</sup> ] | 13.938[b]   | 0.758   | 0.833   | 0.723   | 1.259  |
| <i>F</i> (000)  | 452   | 908   | 820   | 470   | 724  |
| Reflections collected   | 4361  | 3284  | 3106  | 3618  | 2558   |
| Unique reflections <i>I</i> ≥ 2σ( <i>I</i> )                        | 1417  | 3284  | 2938  | 3430  | 1979   |
| <i>R</i>  | 0.035   | 0.036   | 0.038   | 0.029   | 0.046  |
| <i>wR</i>   | 0.083   | 0.097   | 0.086   | 0.080   | 0.112  |

[a] Absolute structure parameter (Flack *x* parameter)<sup>[51]</sup> = −0.005(7). [b] Cu-*K* $\alpha$  radiation.

CCDC-206841, -206842, -206843, -206844 and -206845 contain the supplementary crystallographic data for this paper. These data can be obtained free of charge at [www.ccdc.cam.ac.uk/conts/retrieving.html](http://www.ccdc.cam.ac.uk/conts/retrieving.html) [or from the Cambridge Crystallographic Data Centre, 12 Union Road, Cambridge CB2 1EZ, UK; Fax: (internat.) +44-1223-336-033; E-mail: [deposit@ccdc.cam.ac.uk](mailto:deposit@ccdc.cam.ac.uk)].

## Acknowledgments

Financial support from both the Ministerio de Ciencia y Tecnología (BQU2001–3715) and Junta de Andalucía is gratefully acknowledged. Thanks are expressed to Mr. Dante Masi for technical assistance with the X-ray work carried out at ICCOM and to Professor Davide Proserpio for providing the SCHAKAL picture. We are also grateful to Mr. César J. Pastor Montero (Laboratorio de Difracción de Rayos X, Facultad de Ciencias, Universidad Autónoma de Madrid) for the acquisition of the X-ray diffraction data of complex 1.

**Note Added in Proof** (November 18, 2003): The X-ray structure of an Mn(oda) complex has been reported (C. Jiang, X. Zhu, Z.-P. Yu, Z.-Y. Wang, *Inorg. Chem. Commun.* **2003**, 6, 706) while our work was in progress.

- [1] *Manganese and Its Role in Biological Processes*, in *Metal Ions in Biological Systems* (Eds.: A. Sigel, H. Sigel), Marcel Dekker, New York, **2000**, vol. 37.
- [2] N. A. Law, M. T. Caudle, V. L. Pecoraro, *Adv. Inorg. Chem.* **1999**, 46, 305.
- [3] *Manganese Redox Enzymes* (Ed.: V. L. Pecoraro), VCH, New York, **1992**.
- [4] G. C. Dismukes, *Chem. Rev.* **1996**, 96, 2909.
- [5] V. K. Yachandra, K. Sauer, M. P. Klein, *Chem. Rev.* **1996**, 96, 2927.
- [6] N. Bresciani-Pahor, G. Nardin, R. P. Bonomo, E. Rizzarelli, *J. Chem. Soc., Dalton Trans.* **1983**, 1797.

- [7] U. Thewalt, T. Guthner, *J. Organomet. Chem.* **1989**, 379, 59.
- [8] A. K. Powell, J. M. Charnock, A. C. Flood, C. D. Garner, M. J. Ware, W. Clegg, *J. Chem. Soc., Dalton Trans.* **1992**, 203.
- [9] R. Baggio, M. T. Garland, M. Perec, *J. Chem. Soc., Dalton Trans.* **1996**, 2747.
- [10] R. Baggio, M. T. Garland, M. Perec, *Inorg. Chim. Acta* **2000**, 310, 103.
- [11] D. del Río, A. Galindo, J. Tejero, F. J. Bedoya, A. Ienco, C. Mealli, *Inorg. Chem. Commun.* **2000**, 3, 32.
- [12] A. Gorrane, A. Pastor, A. Ienco, C. Mealli, A. Galindo, *J. Chem. Soc., Dalton Trans.* **2002**, 3771.
- [13] S. H. Whitlow, G. Davey, *J. Chem. Soc., Dalton Trans.* **1975**, 1228.
- [14] R. P. Bonomo, E. Rizzarelli, N. Bresciani-Pahor, G. Nardin, *Inorg. Chim. Acta* **1981**, 54, 17.
- [15] D. del Río, A. Galindo, R. Vicente, C. Mealli, A. Ienco, D. Masi, *Dalton Trans.* **2003**, 1813.
- [16] Cambridge Structural Database System, Cambridge Crystallographic data Centre, 12 Union Road, Cambridge, CB2 1EZ, UK; F. H. Allen, O. Kennard, *Chem. Des. Autom. News* **1993**, 8, 31.
- [17] W. E. Hatfield, J. H. Helms, B. R. Rohrs, P. Singh, J. R. Wasson, R. R. Weller, *Proc. Ind. Acad. Sci., Chem. Sci.* **1987**, 98, 23.
- [18] R. Baggio, M. T. Garland, M. Perec, D. Vega, *Inorg. Chim. Acta* **1999**, 284, 49.
- [19] S. N. Dubey, R. K. Beweja, D. M. Puri, *Indian J. Chem. Sect A* **1983**, 22, 450.
- [20] A. Gorrane, A. Pastor, A. Galindo, A. Ienco, C. Mealli, P. Rosa, *Chem. Commun.* **2003**, 512.
- [21] M. K. Kabir, M. Kawahara, H. Kumagai, K. Adachi, S. Kawata, T. Ishii, S. Kitagawa, *Polyhedron* **2001**, 20, 1417.
- [22] B. Chiswell, D. S. Litster, *Inorg. Chim. Acta* **1978**, 29, 25.
- [23] C. M. Harris, T. N. Lockyer, N. C. Stephenson, *Aust. J. Chem.* **1966**, 19, 1741.
- [24] J. S. Judge, W. M. Reiff, G. M. Intille, P. Ballway, W. A. Baker Jr., *J. Inorg. Nucl. Chem.* **1967**, 29, 1711.
- [25] M. Devereux, M. McCann, V. Leon, V. McKee, R. J. Ball, *Polyhedron* **2002**, 21, 1063.

- [26] R. Baggio, M. T. Garland, M. Perec, D. Vega, *Inorg. Chem.* **1995**, *34*, 1961.
- [27] W. Ma, H. van Koningsveld, J. A. Peters, T. Maschmeyer, *Chem. Eur. J.* **2001**, *7*, 657.
- [28] See for example: *Inorganic Chemistry: Principles of Structure and Reactivity*, J. E. Huheey, E. A. Keiter, R. L. Keiter, 4<sup>th</sup> ed., Harper Collins, New York, **1993**.
- [29] R. D. Shannon, *Acta Crystallogr., Sect. A* **1976**, *32*, 751.
- [30] N. Mangayarkarasi, M. Prabhakar, P. S. Zacharias, *Polyhedron* **2002**, *21*, 925.
- [31] Y. Zhang, S. Wang, C. Bridges, J. E. Greedan, *Can. J. Chem.* **2000**, *78*, 1289.
- [32] L. R. Gahan, V. A. Grillo, T. W. Hambley, G. R. Hanson, C. J. Hawkins, E. M. Proudfoot, B. Moubaraki, K. S. Murray, D. Wang, *Inorg. Chem.* **1996**, *35*, 1039.
- [33] S. Karmakar, S. B. Choudhury, A. Chakravorty, *Inorg. Chem.* **1994**, *33*, 6148.
- [34] P. Chakraborty, S. K. Chandra, A. Chakravorty, *Inorg. Chem.* **1993**, *32*, 5349.
- [35] M. O'Keeffe, M. Eddaoudi, H. Li, T. Reineke, O. M. Yaghi, *J. Solid State Chem.* **2000**, *152*, 3.
- [36] O. Kahn, *Molecular Magnetism*, VCH, New York, **1993**.
- [37] H. Iikura, T. Nagata, *Inorg. Chem.* **1998**, *37*, 4702.
- [38] M. McCann, M. T. Casey, M. Devereux, M. Curran, G. Ferguson, *Polyhedron* **1997**, *16*, 2547.
- [39] Y.-Q. Zheng, J.-L. Lin, J. Sun, Z. Anorg. Allg. Chem. **2001**, *627*, 1059.
- [40] M. J. Plater, M. R. St. J. Foreman, R. A. Howie, *J. Chem. Cryst.* **2000**, *30*, 445.
- [41] L. S. Erre, G. Micera, E. Garribba, A. Cs. Benyei, *New J. Chem.* **2000**, *24*, 725.
- [42] C. J. O'Connor, *Prog. Inorg. Chem.* **1982**, *29*, 20.
- [43] Bruker, Programs SMART, version 5.054; SAINT, version 6.2.9; SADABS version 2.03; XPREP, version 5.1; SHELXTL, version 5.1. Bruker AXS Inc., Madison, WI, USA, **2001**.
- [44] G. M. Sheldrick, Programs SHELXS-97 (crystal structure solution) and SHELXL-97 (crystal structure refinement), University of Göttingen, Germany, **1997**.
- [45] D. T. Cromer, J. T. Waber, *Acta Crystallogr.* **1965**, *18*, 104.
- [46] SIR97, A. Altomare, M. C. Burla, M. Cavalli, G. L. Casciarano, C. Giacovazzo, A. Gagliardi, A. G. G. Moliterni, G. Polidori, R. Spagna, *J. Appl. Cryst.* **1999**, *32*, 115.
- [47] ORTEP-III, M. N. Burnett, C. K. Johnson, Report ORNL-6895. Oak Ridge National Laboratory, Oak Ridge, TN, **1996**.
- [48] L. J. Farrugia, *J. Appl. Chem.* **1997**, *30*, 565.
- [49] E. Keller, *J. Appl. Crystallogr.* **1989**, *22*, 12.
- [50] L. J. Farrugia, *J. Appl. Chem.* **1999**, *32*, 837.
- [51] H. D. Flack, G. Bernardinelli, *Acta Crystallogr., Sect. A* **1999**, *55*, 908.

Received July 24, 2003

Early View Article

Published Online December 12, 2003